

See discussions, stats, and author profiles for this publication at: <https://www.researchgate.net/publication/270219633>

# Controlled Polymerization of N-Substituted Glycine N-Thiocarboxyanhydrides Initiated by Rare Earth Borohydrides toward Hydrophilic and Hydrophobic Polypeptoids

ARTICLE *in* MACROMOLECULES · SEPTEMBER 2014

Impact Factor: 5.8 · DOI: 10.1021/ma501131t

---

CITATIONS

6

---

READS

39

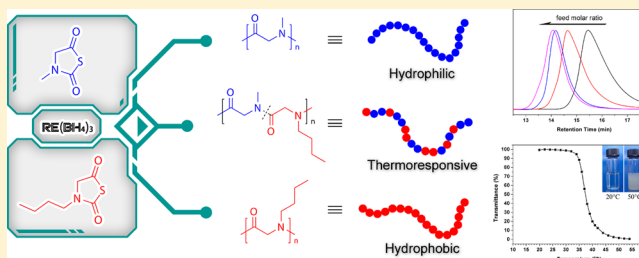
# Controlled Polymerization of N-Substituted Glycine N-Thiocarboxyanhydrides Initiated by Rare Earth Borohydrides toward Hydrophilic and Hydrophobic Polypeptoids

Xinfeng Tao, Yangwei Deng, Zhiquan Shen, and Jun Ling\*

MOE Key Laboratory of Macromolecular Synthesis and Functionalization, Department of Polymer Science and Engineering, Zhejiang University, Hangzhou 310027, China

## S Supporting Information

**ABSTRACT:** N-substituted glycine N-thiocarboxyanhydrides (NTAs) are alternative monomers to prepare polypeptoids with large-scale producing potential compared to the corresponding N-carboxyanhydrides (NCAs) due to their easily synthetic approach and stability during purification and storage. Novel monomer N-butylglycine NTA (NBG-NTA) has been synthesized and well characterized for the first time. Rare earth borohydrides  $[\text{RE}(\text{BH}_4)_3(\text{THF})_3]$ , RE = Sc, Y, La, Nd, Dy, and Lu] have been first applied in the polymerization of sarcosine NTA (Sar-NTA) and NBG-NTA to achieve high molecular weight (MW) hydrophilic and hydrophobic polypeptoids. Polysarcosines (PSars), poly(N-butylglycine)s (PNBGs), and their copolymers with high yields, high MWs, and moderate MW distributions are synthesized at 60 °C by using  $\text{RE}(\text{BH}_4)_3(\text{THF})_3$  initiators. MWs of polypeptoids are controlled by feed molar ratios. For instance, PSar with an absolute  $M_n$  of 27.7 kDa (DP = 390) and PDI of 1.14 is produced successfully from Sar-NTA. Thermoresponsive random copolypeptoids poly(sarcosine-*r*-N-butylglycine)s [P(Sar-*r*-NBG)s] have reversible phase transitions (cloud point temperature) in aqueous solution and minimal cytotoxicity comparable to PEG and PSar, which is promising in various biomedical and biotechnological applications. Thermal properties of homo- and co-polypeptoids are investigated by TGA and DSC measurements.



## INTRODUCTION

Poly( $\alpha$ -peptoid)s, or polypeptoids, are biomaterials possessing N-substituted polyglycine backbones with side groups on the nitrogen atoms. Though having similar structure compared to polypeptides, polypeptoids lack hydrogen bonding along the backbones because of N-substituents, which makes them soluble in many common solvents and amenable to thermal processing.<sup>1–5</sup> The conformations of polypeptoids are controlled by steric hindrance and electronic properties of side groups rather than hydrogen bonding, exhibiting random coils or well-defined secondary structures.<sup>6,7</sup> Oligopeptoids with designed structure have enhanced membrane permeability<sup>8</sup> and proteolytic stability to enzymes<sup>9</sup> compared with oligopeptides but still can be biodegradable through oxidative pathways.<sup>10</sup> Because of the challenge of synthesis and potential in biomedical applications, researchers have been paying increasing attention to polypeptoids.<sup>6,11</sup>

Polypeptoids are mainly prepared by ring-opening polymerization (ROP) of N-substituted glycine N-carboxyanhydride (NCA) monomers.<sup>1,12–14</sup> Zhang and co-workers prepared cyclic homo- and block-polypeptoids,<sup>3,12</sup> as well as cyclic brush-like polypeptoids<sup>15</sup> by using N-heterocyclic carbenes (NHCs) and investigated the polymerization mechanism<sup>16</sup> and physical properties detailedly.<sup>3,5</sup> They also synthesized thermoresponsive linear and cyclic random copolypeptoids<sup>17</sup> and bottlebrush copolypeptoids<sup>18</sup> with tunable cloud point temperatures ( $T_{cp}$ s)

in aqueous solution. Luxenhofer and co-workers carried out living ROP of N-substituted glycine NCAs initiated by primary amines,<sup>1,19</sup> as well as surface-initiated<sup>20</sup> and solid support-initiated<sup>21</sup> polymerizations, to synthesize a series of homo-polypeptoids as well as di- and multiblock co-polypeptoids. They investigated the solubility,<sup>1</sup> thermal property,<sup>4</sup> and biodegradability<sup>10</sup> of the products to enhance comprehensive understanding. Water-soluble and biodegradable polypeptoids were regarded as a competitive alternatives of PEG.<sup>1</sup> Schlaad reported the thermoresponsive poly(N-C3 glycine)s with  $T_{cp}$ s effected by structural and electronic properties of the side groups. Crystalline microparticles of poly(N-(*n*-propyl)glycine) and poly(N-allylglycine) were observed during long-term annealing in aqueous solution.<sup>13</sup>

NCAs must be synthesized and polymerized in extremely anhydrous and anaerobic solutions and apparatuses due to their sensitivity to moisture and heat. Moreover, they cannot be stored for a long period of time and have to be specially purified before use.<sup>22,23</sup> Amino acid N-thiocarboxyanhydrides (NTAs),<sup>24–27</sup> the thio-analogues of NCAs, are much more stable monomers for polypeptoid synthesis with the potential of large-scale production. Kricheldorf and co-workers reported

Received: May 31, 2014

Revised: August 19, 2014

Published: September 10, 2014

a pioneer work on the polymerization of NTAs initiated by primary amine.<sup>28</sup> They thought that it was too hard to prepare high molar mass polypeptides from NTAs by using primary amine initiators because of the low activity of NTA monomers. In our previous work, polysarcosines (PSars) with quantitative yields (>94%), low polydispersity indices (PDIs) (<1.2), and predictable molecular weights (MWs) (when DP < 100) were synthesized from sarcosine NTA (Sar-NTA) initiated by poly(ethylene glycol)amine, which created a more controllable synthetic method toward polypeptides.<sup>29</sup> Synthesis of high MWs (DP > 100) polypeptides from N-substituted glycine NTAs was still a significant and challenging issue requiring highly active initiators.

Rare earth compounds exhibit excellent catalytic properties in ROP of lactones,<sup>30–35</sup> lactides,<sup>36,37</sup> cyclic carbonates,<sup>38–40</sup> cyclic ethers,<sup>41–43</sup> and NCAs as well.<sup>44–47</sup> We have reported polymerization of NCAs initiated by rare earth borohydrides [RE(BH<sub>4</sub>)<sub>3</sub>(THF)<sub>3</sub>] with quantitative yields and high MWs ( $M_n$  = 86.2 kDa).<sup>47</sup> The high catalytic activity of rare earth compounds makes them promising initiators for ROP of NTAs to produce high-MW polypeptides.

In this work, we investigate the controlled ROP of Sar-NTA and *N*-butylglycine NTA (NBG-NTA) initiated by RE-(BH<sub>4</sub>)<sub>3</sub>(THF)<sub>3</sub> (RE = Sc, Y, La, Nd, Dy, and Lu) to produce high-MW hydrophilic and hydrophobic polypeptides. The polymerizations are carried out in selected solvents resulting in high yields, moderate PDIs, and predictable MWs by tuning feed molar ratio of monomer to initiator. Random copolymers poly(sarcosine-*r*-*N*-butylglycine)s [P(Sar-*r*-NBG)s] are also synthesized by ROP of Sar-NTA with NBG-NTA. They are thermoresponsive polymers with reversible phase transitions, known as cloud point temperature ( $T_{cp}$ ), in aqueous solution. The biocompatibility of the copolypeptoid P(Sar-*r*-NBG) is assessed by cell viability assay. Thermal properties of homo- and co-polypeptides are investigated and compared with the data in the literature.

## EXPERIMENTAL SECTION

**Materials.** Sarcosine (98%, Shanghai Adamas Reagent, China), *n*-butylamine (99.5%, J&K Chemical Reagent, China), glyoxylic acid monohydrate (98%, J&K Chemical Reagent, China), carbon disulfide (99%, Sinopharm Chemical Reagent, China), sodium chloroacetate (98%, Shanghai Jingchun, China), and phosphorus tribromide (98.5%, Sinopharm Chemical Reagent, China) were used as received. Dioxane and tetrahydrofuran (THF) were refluxed before use over sodium/benzophenone ketyl and potassium/benzophenone ketyl, respectively. *N,N*-Dimethylformamide (DMF) was stirred over CaH<sub>2</sub> and followed by distillation under reduced pressure. Acetonitrile was stirred over CaH<sub>2</sub> and distilled. RE(BH<sub>4</sub>)<sub>3</sub>(THF)<sub>3</sub> (RE = Sc, Y, La, Nd, Dy, and Lu) was prepared according to the procedure described in the literature<sup>30</sup> and our previous report.<sup>47</sup>

**Synthesis of 5-Ethoxythiocarbonylmercaptoacetic Acid (XAA).** NaOH (30.0 g, 0.75 mol) was dissolved in 150 mL of ethanol and 375 mL of water followed by bubbling argon through the solution for 15 min. Then carbon disulfide (54 mL, 0.90 mol) was added dropwise with stirring at 0 °C. The mixture was reacted for 2 h in an argon atmosphere. Afterward, an aqueous solution of sodium chloroacetate (87.36 g, 0.75 mol) was added to the reaction mixture and stirred at 25 °C. After 24 h, the mixture was acidified by adding concentrated hydrochloric acid and extracted three times with 200 mL of chloroform each. The extracts were dried with Na<sub>2</sub>SO<sub>4</sub> and concentrated in a vacuum. The products were obtained by crystallizing twice in chloroform/hexane and isolated by filtration, which were light yellow crystals (48.7 g, yield 36.1%). <sup>1</sup>H NMR (CDCl<sub>3</sub>/TMS)  $\delta$ : 1.43 ppm (t, 3H), 3.98 ppm (s, 2H), 4.66 ppm (q, 2H).

**Synthesis of Sarcosine NTA (Sar-NTA).** Sarcosine (22.27 g, 0.25 mol), XAA (45.02 g, 0.25 mol), and NaOH (20.82 g, 0.52 mol) were dissolved in 300 mL of water and reacted for 72 h at 25 °C with stirring. Then the reaction mixture was acidified by concentrated hydrochloric acid. The product *N*-ethoxythiocarbonylsarcosine was extracted with chloroform. The organic phase was washed with aqueous citric acid (5 wt %) and concentrated under reduced pressure after drying over Na<sub>2</sub>SO<sub>4</sub>. The remaining product was dissolved in 300 mL of dry chloroform in an argon atmosphere. PBr<sub>3</sub> (30.3 mL, 0.318 mol) was added dropwise in 15 min at 0 °C. The reaction mixture was stirred for an additional 10 min at 0 °C and 1 h at room temperature. After being washed by saturated solution of NaHCO<sub>3</sub> and deionized water, the chloroform solution was dried with MgSO<sub>4</sub> and concentrated in a vacuum. The crude product was purified by column chromatography (ethyl acetate:petroleum ether = 1:3). Light yellow oil was obtained (14.0 g, yield 42.7%) and stored under an argon atmosphere. <sup>1</sup>H NMR (CDCl<sub>3</sub>/TMS)  $\delta$ : 3.11 ppm (s, 3H), 4.21 ppm (s, 2H).

**Synthesis of *N*-Butylglycine Hydrochloride.** Glyoxylic acid monohydrate (72.88 g, 0.792 mol) and *n*-butylamine (39.0 mL, 0.396 mol) were added to 900 mL of CH<sub>2</sub>Cl<sub>2</sub>. After being stirred at 25 °C for 24 h, the solvent was evaporated and 800 mL of hydrochloric acid (2 mol/L) was added. The reaction mixture was refluxed for 12 h. Then the solvent was concentrated. The yellow crude product was recrystallized in methanol/ethyl ether to obtain white crystals (42.77 g, yield 64.4%). <sup>1</sup>H NMR (DMSO-*d*<sub>6</sub>/TMS)  $\delta$ : 0.88 ppm (t, 3H), 1.31 ppm (m, 2H), 1.61 ppm (m, 2H), 2.89 ppm (t, 2H), 3.83 ppm (s, 2H), 9.26 ppm (s, 2H).

**Synthesis of *N*-Butylglycine NTA (NBG-NTA).** NBG-NTA was synthesized by the same procedure of Sar-NTA from *N*-butylglycine hydrochloride. The crude product was purified by column chromatography (ethyl acetate:petroleum ether = 1:7). Yellow oil was obtained (8.5 g, yield 36.1%) and stored under an argon atmosphere. <sup>1</sup>H NMR (CDCl<sub>3</sub>/TMS)  $\delta$ : 0.97 ppm (t, 3H), 1.38 ppm (m, 2H), 1.61 ppm (m, 2H), 3.54 ppm (t, 2H), 4.19 ppm (s, 2H). <sup>13</sup>C NMR (CDCl<sub>3</sub>/TMS)  $\delta$ : 13.65 ppm (CH<sub>3</sub>CH<sub>2</sub>CH<sub>2</sub>CH<sub>2</sub>-), 19.88 ppm (CH<sub>3</sub>CH<sub>2</sub>CH<sub>2</sub>CH<sub>2</sub>-), 29.49 ppm (CH<sub>3</sub>CH<sub>2</sub>CH<sub>2</sub>CH<sub>2</sub>-), 44.02 ppm (CH<sub>3</sub>CH<sub>2</sub>CH<sub>2</sub>CH<sub>2</sub>-), 59.89 ppm (-CH<sub>2</sub>CO-), 164.73 ppm (-NCO-SCO-), 194.26 ppm (-NCOSCO-).

**Polymerizations of Sar-NTA and NBG-NTA Initiated by RE(BH<sub>4</sub>)<sub>3</sub>(THF)<sub>3</sub>.** All polymerizations were performed using the Schlenk technique, and all polymerization tubes were predried and purged with argon.

As a typical homopolymerization, Sar-NTA (0.729 g, 5.56 mmol) was dissolved in 11.5 mL of dry acetonitrile, followed by 0.26 mL of Y(BH<sub>4</sub>)<sub>3</sub>(THF)<sub>3</sub> in THF solution (0.0542 mol/L). The tube was sealed and placed in a 60 °C oil bath for 48 h. The polymer was isolated by precipitation from diethyl ether and dried in a vacuum (0.387 g, 98%).

NBG-NTA (0.372 g, 2.15 mmol) was dissolved in 4.5 mL of dry THF, followed by 0.18 mL of Lu(BH<sub>4</sub>)<sub>3</sub>(THF)<sub>3</sub> in THF solution (0.0572 mol/L). The tube was sealed and placed in a 60 °C oil bath for 48 h. The polymer was isolated by precipitation from diethyl ether and dried in a vacuum (0.190 g, 78.1%).

As a typical random copolymerization, Sar-NTA (0.297 g, 2.26 mmol) and NBG-NTA (0.268 g, 1.55 mmol) were dissolved in 7.6 mL of dry THF, followed by 0.34 mL of Lu(BH<sub>4</sub>)<sub>3</sub>(THF)<sub>3</sub> in THF solution (0.0572 mol/L). The tube was sealed and placed in a 60 °C oil bath for 48 h. The polymer was isolated by precipitation from diethyl ether and dried in a vacuum (0.221 g, 55.5%).

**Measurements.** Molecular weights (MWs) and polydispersity indices (PDIs) were determined by size-exclusion chromatography/multiangle laser light scattering (SEC/MALLS) which consisted of a Waters 1515 isocratic high performance liquid chromatograph pump, a Wyatt DAWN DSP MALLS detector, a Wyatt Optilab DSP interferometric refractometer (RI), and a column of PLgel 5  $\mu$ m MIXED-C. DMF containing 0.05 mol/L LiBr was used as the eluent with a flow rate of 1.0 mL/min at 60 °C. MWs and PDIs were determined by MALLS data and conventional SEC analysis with RI and calibration curve, respectively. Commercial poly(methyl

methacrylate)s were used as the calibration standards. The refractive index increment ( $dn/dc$ ) of the polypeptoids was determined by a Brookhaven BI-DNDC differential refractometer and BI-DNDCW software. The  $dn/dc$  of PSar and PNBG in 0.05 mol/L LiBr/DMF at 25 °C was determined as 0.0931 and 0.0786 mL/g, respectively. Nuclear magnetic resonance (NMR) spectra were recorded on a Bruker Avance DMX 500 spectrometer ( $^1\text{H}$ : 500 MHz) with DMSO- $d_6$  or  $\text{CDCl}_3$  as solvent and tetramethylsilane (TMS) as internal reference. Electrospray ionization mass spectrometry (ESI-MS) spectrum was measured by Varian MS-500 liquid chromatograph mass spectrometer. The hydrodynamic diameters of the nanoparticles were measured by dynamic light scattering (DLS) using a particle size analyzer (Zetasizer Nano Series, Malvern Instruments) at 25 °C. The measurements were made at a fixed angle at 90° and a wavelength of 657 nm. UV–vis spectra were recorded on a UV-2550 UV–vis spectrophotometer (Shimadzu) equipped with a TCC-240A temperature controlled cell holder (Shimadzu). Differential scanning calorimetry (DSC) analyses were performed on a TA Q200 instrument. PSars were heated to 160 °C at a rate of 10 °C/min under a nitrogen purge, held for 3 min to erase the thermal history, cooled to 25 °C at a rate of 20 °C/min, and finally subjected to a second scan. PNBGs and P(Sar-*r*-NBG)s were heated from –25 to 250 °C at a rate of 10 °C/min under a nitrogen purge, held for 3 min to erase the thermal history, cooled to –30 °C at a rate of 20 °C/min, and finally subjected to a second scan. Thermogravimetric analysis (TGA) was performed on a TA Q500 instrument. Samples were heated to 500 °C at a rate of 10 °C/min.

**Cytotoxicity Assay.** HepG2 cells were seeded in 96-well plates with the initial density of 10 000 cells per well and cultured overnight to 80% cell confluence. All polymers were dissolved in 4-(2-hydroxyethyl)-1-piperazineethanesulfonic acid (HEPES) buffer and diluted to appropriate concentrations (14–80  $\mu\text{g/mL}$ ). The polymer/HEPES buffer solution was added to the wells, and the cells were incubated in the incubator for 48 h. The polymer concentration in the well was in the range from 14 to 80  $\mu\text{g/mL}$ . Cell viability was tested with methylthiazolyltetrazolium (MTT) assay. Briefly, the medium was replaced by solution containing 20  $\mu\text{L}$  of MTT, and the cells were incubated for 4 h. Then, the medium was removed, and 200  $\mu\text{L}$  of dimethyl sulfoxide (DMSO) was added to dissolve the generated formazan. The plates were shaken for 15 min before the detection with a microplate reader (550, Bio-Rad) at 570 nm. A total of five replicates were conducted for each treatment.

## RESULTS AND DISCUSSION

**Monomer Synthesis.** Sar-NTA is prepared according to the procedure described in the literature<sup>28</sup> and our previous work<sup>29</sup> (Scheme S1 in Supporting Information) and confirmed by  $^1\text{H}$  NMR (Figure S1). We report NBG-NTA for the first time (Scheme S2) from *N*-butylglycine hydrochloride.<sup>48</sup> The structure of NBG-NTA monomer is well characterized by  $^1\text{H}$  NMR,  $^{13}\text{C}$  NMR,  $^1\text{H}$ – $^1\text{H}$  COSY, and  $^1\text{H}$ – $^{13}\text{C}$  HMQC (Figures S2–S5) spectra. The signal of methyl protons of the *n*-butyl side group is found at 0.97 ppm (t,  $\text{H}^a$ ), and methylene protons on side group appear at 1.38 ppm (m,  $\text{H}^b$ ), 1.61 ppm (m,  $\text{H}^c$ ), and 3.54 ppm (t,  $\text{H}^d$ ). The signal at 4.19 ppm (s,  $\text{H}^e$ ) is assigned to methylene protons on five-membered ring. The methyl signal  $\text{H}^a$  is coupled with signal  $\text{H}^b$  (inset C in Figure S4). Likewise, two methylene signals  $\text{H}^b$  and  $\text{H}^c$  on the *n*-butyl side group are coupled with protons on adjacent carbons (insets A and B in Figure S4). ESI-MS spectrometry of NBG-NTA shows a peak at 174.0  $m/z$  generated by (NBG-NTA) $\text{H}^+$ . All the syntheses are conducted in open air. It is much easier to prepare *N*-substituted glycine NTA than NCA analogues. The liquid NTA monomers can be stored in an argon atmosphere at room temperature for several months to a year without any decomposition or oligomerization. Easy synthesis and long

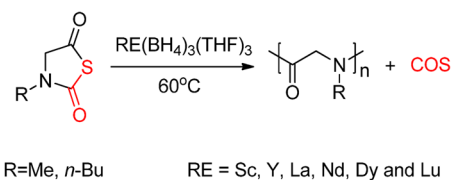
shelf-time make NTA monomers suitable commercial products to prepare polypeptoids.

**Polymerization Features.** In order to synthesize high-MW PSars from Sar-NTA, we have to solve two problems, i.e., low activity of Sar-NTA monomer and poor solubility of PSar polymer in most common organic solvents.<sup>1,29</sup> We carried out Sar-NTA ROP using  $\text{Y}(\text{BH}_4)_3(\text{THF})_3$  as initiator in various solvents to select optimal reaction medium (Table S1). Although DMF is a standard reaction solvent for polymerizations of NCAs, it is not suitable for NTAs. Sar-NTA polymerizations in DMF at 20 °C (S1 in Table S1) result in only low-MW products with a low yield of 43.2%, which is consistent with our previous report of primary amine-initiated polymerizations of Sar-NTA.<sup>29</sup> It is necessary to increase temperature due to the low reactivity of NTA, but it does not work in this case. When the polymerization temperature is elevated to 60 °C (S2 in Table S1), the yield is still low (48.1%) and MW of the product is too low to be distinguished from the solvent in SEC. DMF can react with growing peptide chains to form aldehyde groups, which terminates the polymerization.<sup>49</sup> DMF also slightly decomposes at 60 °C to dimethylamine and then initiates the polymerization to yield low-MW products.<sup>26,27,49</sup> Sar-NTA polymerizations in dioxane (S3–S6 in Table S1) achieve a more acceptable yield (>70%) but not in a controlled way as the  $M_n$ s of PSars increase slightly from 10.4 to 13.5 kDa when feed molar ratios of monomer to initiator ( $[\text{Sar}]/[\text{Y}]$ ) increase from 49 to 406. The uncontrollability is attributed to the poor solubility of PSar in dioxane, which leads to precipitation during the polymerization. The heterogeneous reaction in dioxane confines the active chain end to react with monomers, limiting MW of PSar and broadening PDI. What encourages us is that PSars initiated by  $\text{Y}(\text{BH}_4)_3(\text{THF})_3$  show higher MWs than those by primary amine initiators.<sup>28,29</sup> In short, neither DMF nor dioxane is an appropriate reaction solvent for Sar-NTA polymerization.

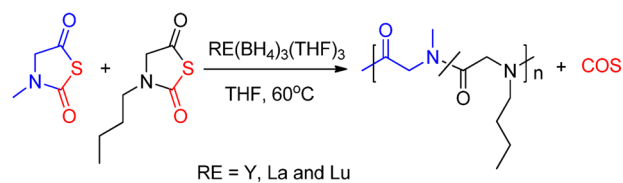
Acetonitrile, a good solvent for PSar, is an appropriate polymerization medium. The results of Sar-NTA ROPs initiated by  $\text{Y}(\text{BH}_4)_3(\text{THF})_3$  in acetonitrile (Scheme 1) are summarized in Table 1. Without precipitation or turbidness, polymerizations of Sar-NTA initiated by  $\text{Y}(\text{BH}_4)_3(\text{THF})_3$  at 60 °C for 48 h with various feed molar ratios of  $[\text{Sar}]/[\text{Y}]$  from 98 to 516 (1–4 in Table 1) exhibit quantitative yields (>90%) and moderate PDIs (1.26–1.40). All SEC traces of the products are

**Scheme 1.** Polymerization of Sar-NTA and NBG-NTA Initiated by  $\text{RE}(\text{BH}_4)_3(\text{THF})_3$

### Homopolymerization



### Copolymerization



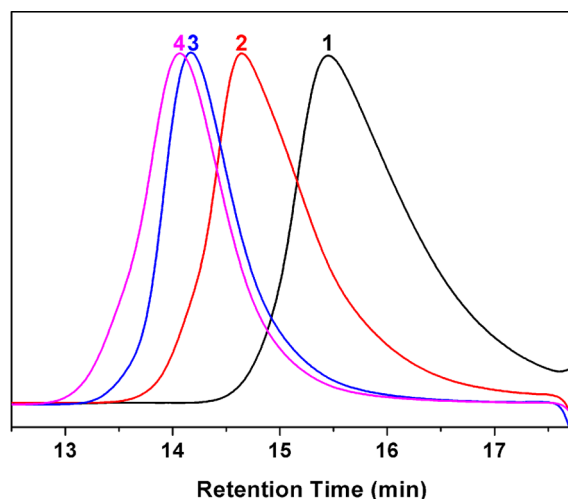


**Table 1.** Polymerization of Sar-NTA in Acetonitrile Initiated by  $Y(BH_4)_3(THF)_3^a$ 

sample	[Sar]/[Y]	temp (°C)	yield (%)	$M_{n,theo}^b$ (kDa)	$M_{n,RI}^c$ (kDa)	PDI <sup>c</sup>	$M_{n,LS}^d$ (kDa)	PDI <sup>d</sup>
1	98	60	84.1	5.9	6.7	1.34		
2	202	60	92.4	13.3	14.6	1.40	12.2	1.12
3	395	60	98.0	27.5	27.1	1.30	22.5	1.09
4	516	60	>99	36.7	34.6	1.26	27.7	1.14
5	168	25	20.5	2.4	3.3	1.18		
6	180	40	68.7	8.8	6.3	1.25		

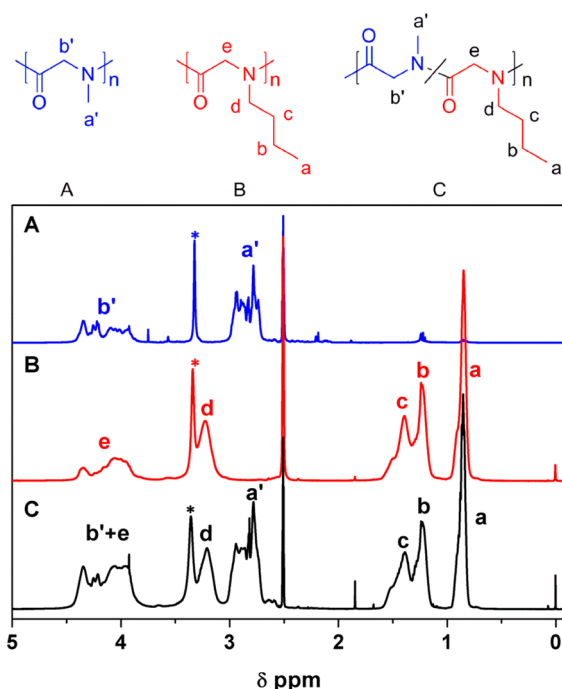
<sup>a</sup>Polymerization conditions: [Sar] = 0.5 mol/L, 48 h in acetonitrile. <sup>b</sup>Theoretical  $M_n$ ,  $M_{n,theo} = [Sar]/[Y] \times \text{yield} \times 71$ . <sup>c</sup>Determined by SEC measurement with interferometric refractometer. <sup>d</sup>Determined by SEC measurement with MALLS detector ( $dn/dc = 0.0931 \text{ mL/g}$ ).

unimodal as shown in Figure 1 and Figure S6 detected by RI and MALLS detectors, respectively. According to SEC/MALLS

**Figure 1.** SEC traces of 1–4 detected by interferometric refractometer.

analyses, products 2–4 with feed molar ratio of 202, 395, and 516 have absolute  $M_n$ s of 12.2, 22.5, and 27.7 kDa, respectively. The absolute  $M_n$ s of products 2–4 are lower than the corresponding theoretical ones because the  $Y(BH_4)_3(THF)_3$  can initiate more than one propagating chain.<sup>30,47</sup> The structure of the obtained product has been confirmed by  $^1H$  NMR in DMSO- $d_6$  (Figure 2A). The protons in PSar backbone ( $H^{a'}$ : 2.65–3.05 ppm;  $H^{b'}$ : 3.85–4.45 ppm) are well identified. This is the first time to produce hydrophilic PSars with  $M_n$ s higher than 10 kDa by Sar-NTA which can replace those obtained from Sar-NCA and suitable for application as biopolymers.<sup>7,11,14</sup>

When polymerization temperature decreases to 40 and 25 °C (5 and 6 in Table 1), PSar yields decrease to 68.7% and 20.5% and  $M_n$ s drop to 6.3 and 3.3 kDa (Figure S7), respectively. Therefore, it is necessary to carry out NTA polymerization at 60 °C to reach quantitative yields, in accordance with the case of primary amine initiators.<sup>29</sup> The other five rare earth borohydride complexes, i.e.,  $RE(BH_4)_3(THF)_3$  where RE = Sc, La, Nd, Dy, and Lu, are investigated as initiators for Sar-NTA ROP. All of them are more efficient than primary amines.<sup>28,29</sup> At comparable molar ratios of [Sar]/[RE] (S7–S11 in Table S2), they produce PSars with  $M_n$ s between 5.2 and 7.0 kDa and the yields between 59.9% and 78.6%, which is not as good as  $Y(BH_4)_3(THF)_3$  though. This relates to the differences of atomic radii and electronic structures of rare earth metals, and yttrium is the most appropriate one. Unimodal SEC

**Figure 2.**  $^1H$  NMR spectra of 1 (A), 7 (B), and 13 (C) in DMSO- $d_6$  (\*: water).

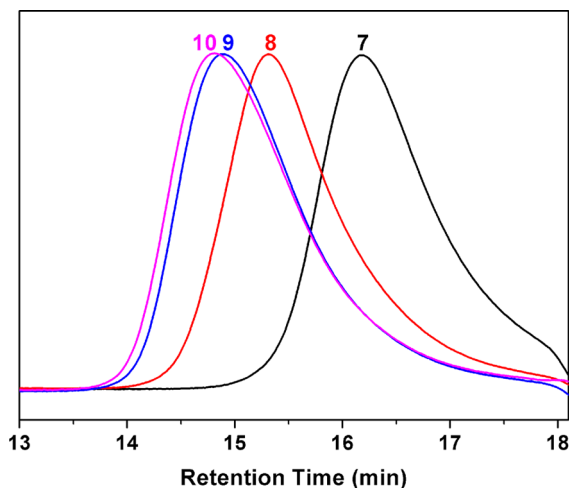
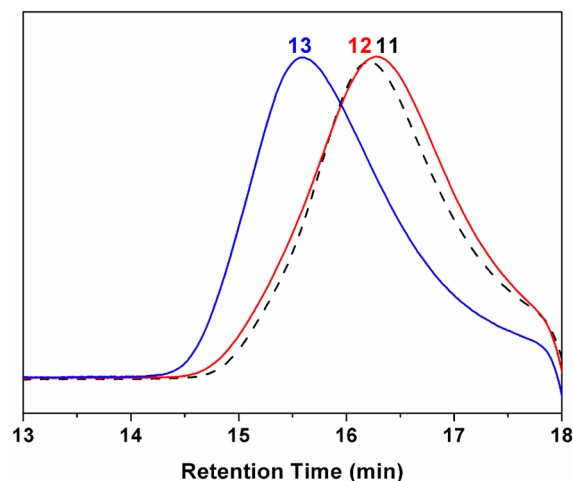
traces of the products (Figure S8) suggest that every reaction has only one active species during polymerization.

We expand rare earth borohydrides to synthesize polypeptoid from another monomer *N*-butylglycine *N*-thiocarboxyanhydride (NBG-NTA). It is the first report of this new monomer despite its NCA analogue (NBG-NCA) having been noticed recently.<sup>1,12,13</sup> The corresponding poly(*N*-butylglycine) (PNBG) product is hydrophobic and soluble in many organic solvents, e.g., THF and chloroform, differing from PSar. Polymerizations of NBG-NTA initiated by  $Lu(BH_4)_3(THF)_3$  were carried out in THF at 60 °C for 48 h (Scheme 1) with the results summarized in Table 2. The yields are higher than 75%, and PDIs of PNBGs are moderate (1.22–1.42) (7–9 in Table 2).  $M_n$ s increase from 3.8 to 10.8 kDa detected by SEC measurement where RI detector underestimates the  $M_n$ s in Table 2. When [NBG]/[Lu] increases to 381 (10 in Table 2), the yield decreases to 65.3% and  $M_n$  (10.7 kDa) remains the same as sample 9, which suggests a good controllability of NBG-NTA ROP only when [NBG]/[Lu] is no higher than 300. All SEC traces of the products are shown in Figure 3 and Figure S9. According to SEC/MALLS analyses, products 8–10 with feed [NBG]/[Lu] ratio of 209, 306, and 381 have absolute  $M_n$ s of 13.7, 21.5, and 23.1 kDa, respectively, lower than the corresponding theoretical ones due to  $Lu(BH_4)_3(THF)_3$

**Table 2.** Polymerization of NBG-NTA in THF Initiated by  $\text{Lu}(\text{BH}_4)_3(\text{THF})_3$ <sup>a</sup>

sample	[NBG]/[Lu]	yield (%)	$M_{n,\text{theo}}^b$ (kDa)	$M_{n,\text{RI}}^c$ (kDa)	PDI <sup>c</sup>	$M_{n,\text{LS}}^d$ (kDa)	PDI <sup>d</sup>
7	98	74.6	8.3	3.8	1.22		
8	209	78.1	18.4	7.4	1.40	13.7	1.04
9	306	80.2	27.7	10.8	1.42	21.5	1.13
10	381	65.3	28.1	10.7	1.51	23.1	1.10

<sup>a</sup>Polymerization conditions: [NBG] = 0.5 mol/L, 48 h in THF at 60 °C. <sup>b</sup>Theoretical  $M_n$ ,  $M_{n,\text{theo}} = [\text{NBG}]/[\text{Lu}] \times \text{yield} \times 113$ . <sup>c</sup>Determined by SEC measurement with interferometric refractometer. <sup>d</sup>Determined by SEC measurement with MALLS detector ( $dn/dc = 0.0786 \text{ mL/g}$ ).

**Figure 3.** SEC traces of 7–10 detected by an interferometric refractometer.**Figure 4.** SEC traces of 11–13 detected by an interferometric refractometer.

initiates more than one propagating chain.<sup>30,47</sup> The structure of the obtained product has been confirmed by  $^1\text{H}$  NMR analysis in  $\text{DMSO}-d_6$  (Figure 2B). The protons of PNBG backbone ( $\text{H}^a$ : 0.84 ppm;  $\text{H}^b$ : 1.23 ppm;  $\text{H}^c$ : 1.39 ppm;  $\text{H}^d$ : 3.22 ppm;  $\text{H}^e$ : 3.80–4.45 ppm) are clearly assigned. Thus, high-MW hydrophobic PNBGs are synthesized successfully from NBG-NTA using  $\text{Lu}(\text{BH}_4)_3(\text{THF})_3$  initiator.

Random copolymerizations of Sar-NTA with NBG-NTA are carried out by  $\text{RE}(\text{BH}_4)_3(\text{THF})_3$  ( $\text{RE} = \text{Y, La, and Lu}$ ) initiators in THF (Scheme 1 and 11–13 in Table 3). To the best of our knowledge, the polymer P(Sar-*r*-NBG) is synthesized for the first time. Neither precipitation nor gelation is observed during the polymerization, which indicates that P(Sar-*r*-NBG) has good solubility in THF differing from PSar. Copolymers are obtained with moderate yields (55.5–69.7%) and moderate PDIs (1.30–1.40), which also reveals unimodal SEC traces (Figure 4).  $^1\text{H}$  NMR analysis indicates that the products are constituted by sarcosine and *N*-butylglycine units based on the clearly distinguished signals (Figure 2C). Methyl proton signals of sarcosine units ( $\text{H}^{a'}$ ) appear in a broad range from 2.67 to 3.06 ppm, while those of *N*-butylglycine units ( $\text{H}^a$ ) present at 0.85 ppm. The methylene proton signals on side groups are detected at 1.23 ppm ( $\text{H}^b$ ), 1.39 ppm ( $\text{H}^c$ ), and

3.20 ppm ( $\text{H}^d$ ). The methylene protons on backbone of both units ( $\text{H}^{b'}$  and  $\text{H}^e$ ) overlap in the range from 3.74 to 4.50 ppm. Based on the intensities of characteristic methyl proton signals of  $\text{H}^a$  and  $\text{H}^{a'}$ , the molar percentage of *N*-butylglycine units in copolymer (NBG mol % in Table 3) is calculated by eq 1.

$$\text{NBG mol \%} = \frac{I(\text{H}^a)}{I(\text{H}^a) + I(\text{H}^{a'})} \times 100\% \quad (1)$$

where  $I(\text{H})$  is integral intensity of the corresponding proton. NBG fractions calculated by NMR are close to the values in feeding when yields are still low (55–70%), indicating Sar-NTA and NBG-NTA have comparable activities. The random structures are also proved by DSC and self-assembly behavior below.

**Polymerization Kinetics.** We investigated polymerization kinetics of Sar-NTA and NBG-NTA with the results summarized in Figures S10 and S11. Polymerization kinetics of Sar-NTA were measured at 60 °C with a feed molar ratio of 150 ( $[\text{Sar-NTA}]/[\text{Y}(\text{BH}_4)_3(\text{THF})_3]$ ) in both sealed tubes and open systems under argon flow using acetonitrile as solvent and  $\text{Y}(\text{BH}_4)_3(\text{THF})_3$  as initiator.  $^1\text{H}$  NMR spectra were collected every 4 h by taking a small amount of reaction mixture and dissolving in  $\text{DMSO}-d_6$ . Monomer conversions were calculated

**Table 3.** Random Copolymerization of Sar-NTA with NBG-NTA Initiated by  $\text{RE}(\text{BH}_4)_3(\text{THF})_3$ <sup>a</sup>

sample	initiator	$[\text{Sar}]/[\text{NBG}]/[\text{RE}]$ (NBG mol %)	yield (%)	$M_{n,\text{RI}}^b$ (kDa)	PDI <sup>b</sup>	NBG <sup>c</sup> (mol %)
11	$\text{Y}(\text{BH}_4)_3(\text{THF})_3$	124/79/1 (38.9)	62.3	4.0	1.30	40.7
12	$\text{La}(\text{BH}_4)_3(\text{THF})_3$	124/95/1 (43.4)	69.7	3.9	1.34	38.6
13	$\text{Lu}(\text{BH}_4)_3(\text{THF})_3$	117/80/1 (40.6)	55.5	5.8	1.40	40.6

<sup>a</sup>Polymerization conditions:  $[\text{Sar}] + [\text{NBG}] = 0.5 \text{ mol/L}$ , 48 h in THF at 60 °C. <sup>b</sup>Determined by SEC measurement with interferometric refractometer. <sup>c</sup>Calculated by  $^1\text{H}$  NMR analyses.

from the relative integration of the methylene proton resonance of Sar-NTA and PSar. Both  $\ln(M_0/M_t)$  vs time plots of the two systems are linear with monomer conversions less than 60%. The polymerization of Sar-NTA under open systems is faster than that in sealed tubes. The liberation of COS gas has an effect on the polymerization of Sar-NTA though it still remains uncertain. The reason can be that the dissolved COS competes with NTA monomer to react with the RE-NMe-polymer chain end. A similar question is also under debate for NCA polymerizations.

Polymerization kinetics of NBG-NTA were measured at the same conditions using THF as solvent and  $\text{Lu}(\text{BH}_4)_3(\text{THF})_3$  as initiator (Figure S11). The polymerization rate of NBG-NTA in THF is lower than the case of Sar-NTA in acetonitrile because of the lower polarity of THF. Similar to the Sar-NTA cases, NBG-NTA polymerizations exhibit linear  $\ln(M_0/M_t)$  vs time plots when the conversions are below 40%. The polymerization rate is also faster under open systems. But the difference is not as much as that of Sar-NTA, which may relate to the solubility of COS in the solvents with difference polarities. Polymerizations of Sar-NTA and NBG-NTA are much slower than the corresponding NCAs.<sup>1,16</sup>

In addition, we measure low-MW products by FTIR analysis to verify whether thiocarbonyl (COS) is still attached to polymer chain ends or not. Two characteristic stretching vibrations of Sar-NTA monomer can be distinguished in Figure S12A with the frequencies at  $1741\text{ cm}^{-1}$  assigned to a-CO and  $1700\text{ cm}^{-1}$  to b-CO. The reduced frequency of b-CO compared with a-CO is caused by the nitrogen electron pair delocalized onto a-CO. This assignment has been demonstrated for NCA monomers.<sup>47</sup> The low-MW PSar sample only arises a characteristic stretching vibration of amide carbonyl (c-CO) with the frequency at  $1663\text{ cm}^{-1}$  (Figure S12B). The disappearance of absorption bands of a-CO and b-CO indicates that there is no thiocarbonyl (COS) attached to polymer chain ends. The FTIR spectra of NBG-NTA and low-MW PNBG sample show similar results (Figure S13). Therefore, we do not have proof to conclude that the liberation of COS is slow.

**Thermal Properties.** We use TGA and DSC analyses to investigate the thermal properties of homo- and co-poly-peptoids. Decomposition temperatures ( $T_{\text{ds}}$ ) of PSar (sample 2), PNBG (sample 7), and P(Sar-*r*-NBG) (sample 13) are 253, 239, and 247 °C (Figure 5), respectively. DSC profiles show that PSar (sample 2) has a glass transition temperature ( $T_g$ )

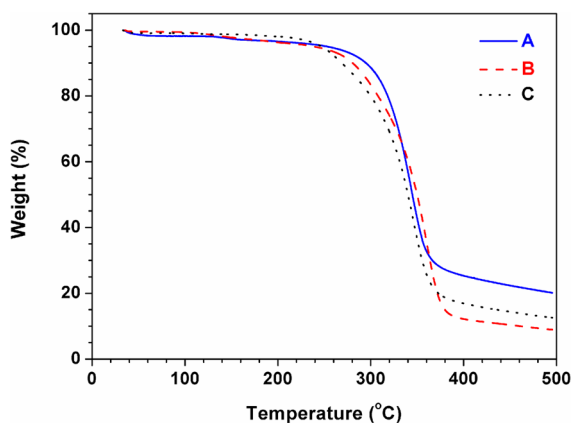


**Figure 5.** TGA profiles of PSar 2 (A), PNBG 7 (B), and P(Sar-*r*-NBG) 13 (C).

around 98 °C (Figure 6A), which is lower than the reported value (143 °C).<sup>4</sup> It may attributed to that sample 2 has a

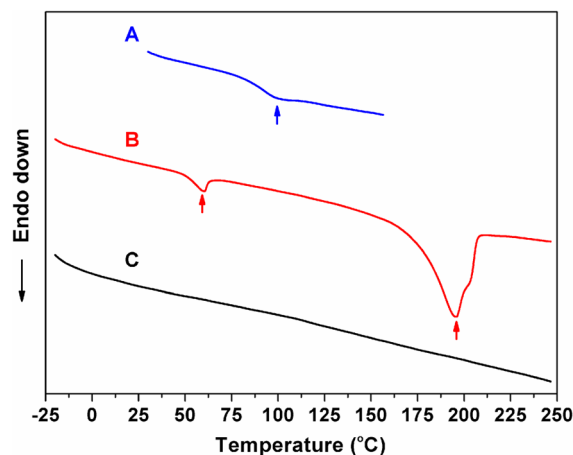


**Figure 6.** DSC profiles of PSar 2 (A), PNBG 7 (B), and P(Sar-*r*-NBG) 13 (C).

broader MW distribution than the reported PSar, and low-MW chains act as plasticizer to decrease  $T_g$ . PNBG (sample 7) exhibits two melting temperatures ( $T_m$ s) at 60 and 196 °C (Figure 6B) with corresponding melting enthalpies ( $\Delta H_m$ s) of 2.3 and 35.6 J/g, respectively.  $T_m$ s of PNBG are slightly lower than the data (70 and 225 °C) reported by Luxenhofer,<sup>4</sup> indicating a lower degree of crystallinity of our sample. However, they are quite different from the values (−65 and 227 °C) reported by Zhang.<sup>5</sup> The second melting enthalpy (35.6 J/g) of our sample is lower than Zhang's result (48 J/g),<sup>5</sup> which also suggests a lower degree of crystallinity of our sample. There is no detectable thermal transition temperature ( $T_g$  or  $T_m$ ) in the DSC profile of P(Sar-*r*-NBG) (sample 13) (Figure 6C), which further supports that P(Sar-*r*-NBG) is a random copolymer.

**Response of P(Sar-*r*-NBG) to Thermal Stimuli.** Homo- and co-poly-peptoids could be thermoresponsive materials with tunable  $T_{\text{cp}}$ .<sup>13,17,18</sup> As an attractive water-soluble polypeptoid, PSar does not exhibit detectable  $T_{\text{cp}}$  by turbidity measurements below 100 °C and appears to be miscible with water in all ratios (for DP < 100).<sup>1</sup> Contributing to the water-insoluble property of PNBG, P(Sar-*r*-NBG)s are thermally responsive and exhibit reversible phase transitions with tunable  $T_{\text{cp}}$  in aqueous solution by controlling NBG fraction in composition. Aqueous solution of sample 13 becomes cloudy upon heating and gets transparent again upon cooling illustrated by the photo in Figure 7 inset, suggesting reversible phase transitions. Turbidity of dilute aqueous solution of 13 is determined by variable UV–vis spectroscopy without stirring. The  $T_{\text{cp}}$  (defined as the temperature at 50% UV–vis transmittance at the light wavelength  $\lambda = 450\text{ nm}$ ) of P(Sar-*r*-NBG) with a concentration of 3.0 mg/mL is 37.4 °C (Figure 7). The transition temperature window ( $\Delta T$ ) (corresponding to the temperature difference at 99% and 1% transmittance) is quite broad (22.6 °C) compared to the random copolymers poly[2-(2-methoxyethoxy)ethyl methacrylate-*co*-oligo(ethylene glycol) methacrylate] [P-(MEO<sub>2</sub>MA-*co*-OEGMA)]<sup>50</sup> and poly[(2-*n*-propyl-2-oxazoline)-*r*-(2-ethyl-2-oxazoline)] [P(*n*PrOx-*r*-EtOx)] ( $\Delta T < 5\text{ °C}$ ),<sup>51,52</sup> while this result is similar to the cases of reported cyclic and linear P(*N*-ethylglycine-*r*-*N*-butylglycine)s [P(NEG-*r*-N BG)s] ( $\Delta T = 10\text{--}18\text{ °C}$ ).<sup>17</sup> Dependence of aggregation size

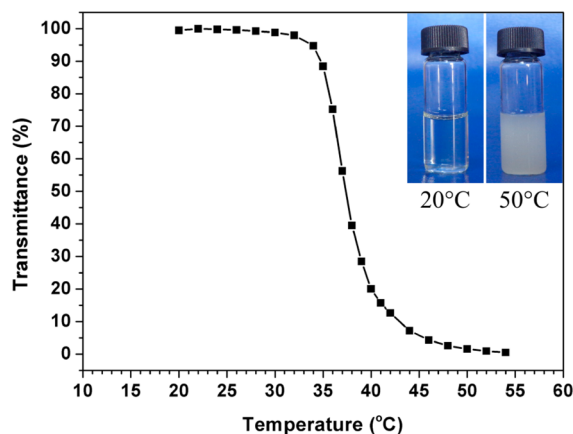


**Figure 7.** Plots of transmittance at  $\lambda = 450$  nm versus temperature for the aqueous solution of P(Sar-*r*-NBG) 13 at a concentration of 3.0 mg/mL. Inset: photographs of sample 13 aqueous solution at 20 and 50 °C.

versus temperature for aqueous solution of 13 (3.0 mg/mL) is determined by DLS measurement as shown in Figure 8 and

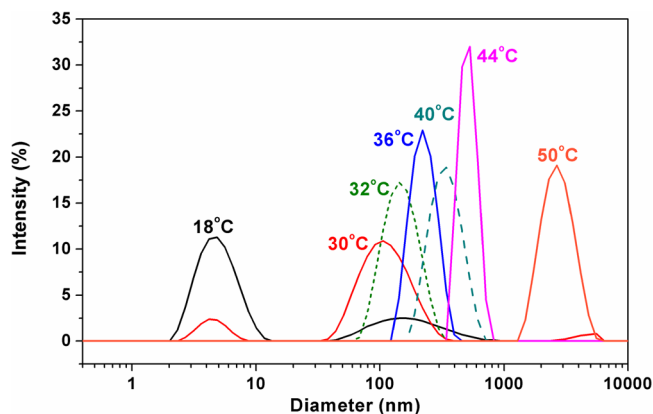


**Figure 8.** DLS profiles of P(Sar-*r*-NBG) 13 aqueous solution at different temperatures at a concentration of 3.0 mg/mL.

Figure S14. P(Sar-*r*-NBG) chains are mainly unimers in dilute aqueous solution at low temperature (Figure 8, 18 °C) with partial aggregations. These aggregations existing below  $T_{cp}$  broaden the effective particle sizes, which results in the broad  $T_{cp}$  transition.<sup>17</sup> When the temperature is elevated to 32 °C, stable nanoparticles (135 nm, PDI = 0.127) are formed due to the hydrophobic interaction-driving aggregation of P(Sar-*r*-NBG) chains. Diameters of aggregations increase gradually with the increasing temperature until copolymer chains precipitate from water. When cooled down, the precipitate redissolves and the aqueous solution turns back to being transparent.

Furthermore, the biocompatibility of the copolypeptoid P(Sar-*r*-NBG) is assessed by using MTT cell viability assay. Human hepatoma (HepG2) cells are incubated for 48 h in HEPES buffers containing sample 13 with different concentrations. Sample 13 (3 mg/mL) has a  $T_{cp}$  around human body temperature. The aggregation of sample 13 at 37 °C leads to the changing of cytotoxicity. The copolypeptoid P(Sar-*r*-NBG) exhibits negligible cytotoxicity at low concentrations (14–80  $\mu$ g/mL) for the good solubility, which is comparable to poly(ethylene glycol) (PEG,  $M_n = 6000$ ) and PSar (sample 2) (Figure 9). The biocompatibility of PSar has not been hindered

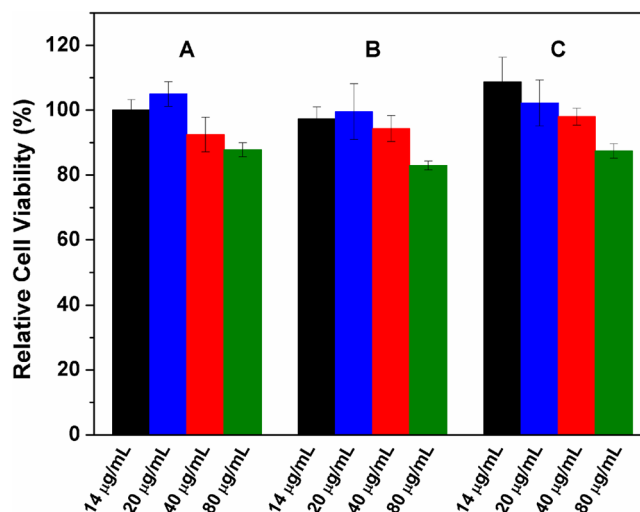


**Figure 9.** Relative cell viability of PEG6K (A), PSar (sample 2) (B), and P(Sar-*r*-NBG) (sample 13) (C) for HepG2 cells after 48 h incubation at a concentration of 14, 20, 40, and 80  $\mu$ g/mL.

by the additional *N*-butylglycine units. The cytotoxicity of P(Sar-*r*-NBG) is similar to the copolypeptoid P(NEG-*r*-NBG) reported by Zhang.<sup>17</sup> However, when the concentration is higher than 1 mg/mL, the copolypeptoid P(Sar-*r*-NBG) exhibits a little cytotoxicity compared to PEG ( $M_n = 6000$ ) and PSar (sample 2) (Figure S15). In this case, sample 13 precipitates from the solution during the assay at high concentration. The solid precipitates are responsible to the increasing of cytotoxicity.

## CONCLUSION

We have carried out a controlled ROP of *N*-substituted glycine NTA initiated by  $\text{RE}(\text{BH}_4)_3(\text{THF})_3$  for the first time to develop a versatile and practical synthetic method to prepare high-MW hydrophilic and hydrophobic polypeptoids. Sar-NTA polymerizations with high yields (>90%) succeeded by using  $\text{Y}(\text{BH}_4)_3(\text{THF})_3$  in acetonitrile, and the MWs of PSar were designable by tuning the feed ratios of [Sar]/[Y]. PSar with an absolute  $M_n$  of 27.7 kDa ( $\text{DP} = 390$ ,  $\text{PDI} = 1.14$ ) was synthesized. This length was comparable to those prepared from Sar-NCA. We prepared and characterized NBG-NTA and used it as the monomer to produce PNBGs initiated by  $\text{Lu}(\text{BH}_4)_3(\text{THF})_3$  in THF. P(Sar-*r*-NBG)s were also obtained by copolymerization of Sar-NTA with NBG-NTA. Thermal properties of homo- and co-polypeptoids were detailedly investigated by TGA and DSC measurements. P(Sar-*r*-NBG)s are thermoresponsive materials exhibiting reversible phase transitions ( $T_{cp}$ ) in aqueous solution. With low cytotoxicity as PEG and PSar, P(Sar-*r*-NBG)s are promising for various biomedical and biotechnological applications. Easy accessibility of NTA monomers paves the way for large-scale industrial production of homo- and co-polypeptoids with high MW.

## ASSOCIATED CONTENT

### Supporting Information

Polymerization data,  $^1\text{H}$  NMR,  $^{13}\text{C}$  NMR,  $^1\text{H}$ – $^1\text{H}$  COSY, and  $^1\text{H}$ – $^{13}\text{C}$  HMQC spectra, SEC curves, polymerization kinetics plots, FT-IR spectra, cytotoxicity assay, and plots of aggregations size vs temperature measured by DLS. This material is available free of charge via the Internet at <http://pubs.acs.org>.



## ■ AUTHOR INFORMATION

## Corresponding Author

\*Tel +86-571-87953739; Fax +86-571-87951773; e-mail lingjun@zju.edu.cn (J.L.).

## Notes

The authors declare no competing financial interest.

## ■ ACKNOWLEDGMENTS

Financial support from the National Natural Science Foundation of China (21174122) is acknowledged. We thank Prof. Youxiang Wang (Zhejiang University) for cytotoxicity analysis.

## ■ REFERENCES

- (1) Fetsch, C.; Grossmann, A.; Holz, L.; Nawroth, J. F.; Luxenhofer, R. *Macromolecules* **2011**, *44* (17), 6746–6758.
- (2) Rosales, A. M.; Murnen, H. K.; Zuckermann, R. N.; Segalman, R. A. *Macromolecules* **2010**, *43* (13), 5627–5636.
- (3) Lee, C. U.; Smart, T. P.; Guo, L.; Epps, T. H.; Zhang, D. H. *Macromolecules* **2011**, *44* (24), 9574–9585.
- (4) Fetsch, C.; Luxenhofer, R. *Polymers* **2013**, *5* (1), 112–127.
- (5) Lee, C. U.; Li, A.; Ghale, K.; Zhang, D. H. *Macromolecules* **2013**, *46* (20), 8213–8223.
- (6) Zhang, D. H.; Lahasky, S. H.; Guo, L.; Lee, C. U.; Lavan, M. *Macromolecules* **2012**, *45* (15), 5833–5841.
- (7) Sun, J.; Zuckermann, R. N. *ACS Nano* **2013**, *7* (6), 4715–4732.
- (8) Kwon, Y. U.; Kodadek, T. *J. Am. Chem. Soc.* **2007**, *129* (6), 1508–1509.
- (9) Patch, J. A.; Barron, A. E. *Curr. Opin. Chem. Biol.* **2002**, *6* (6), 872–877.
- (10) Ulbricht, J.; Jordan, R.; Luxenhofer, R. *Biomaterials* **2014**, *35*, 4848–4861.
- (11) Luxenhofer, R.; Fetsch, C.; Grossmann, A. *J. Polym. Sci., Polym. Chem.* **2013**, *51* (13), 2731–2752.
- (12) Guo, L.; Zhang, D. H. *J. Am. Chem. Soc.* **2009**, *131* (50), 18072–18074.
- (13) Robinson, J. W.; Secker, C.; Weidner, S.; Schlaad, H. *Macromolecules* **2013**, *46* (3), 580–587.
- (14) Birke, A.; Huesmann, D.; Kelsch, A.; Weilbacher, M.; Xie, J.; Bros, M.; Bopp, T.; Becker, C.; Landfester, K.; Barz, M. *Biomacromolecules* **2014**, *15* (2), 548–557.
- (15) Lahasky, S. H.; Serem, W. K.; Guo, L.; Garino, J. C.; Zhang, D. H. *Macromolecules* **2011**, *44* (23), 9063–9074.
- (16) Guo, L.; Lahasky, S. H.; Ghale, K.; Zhang, D. H. *J. Am. Chem. Soc.* **2012**, *134* (22), 9163–9171.
- (17) Lahasky, S. H.; Hu, X. K.; Zhang, D. H. *ACS Macro Lett.* **2012**, *1* (5), 580–584.
- (18) Lahasky, S. H.; Lu, L.; Huberty, W. A.; Cao, J. B.; Guo, L.; Garino, J. C.; Zhang, D. H. *Polym. Chem.* **2014**, *5* (4), 1418–1426.
- (19) Fetsch, C.; Luxenhofer, R. *Macromol. Rapid Commun.* **2012**, *33* (19), 1708–1713.
- (20) Schneider, M.; Fetsch, C.; Amin, I.; Jordan, R.; Luxenhofer, R. *Langmuir* **2013**, *29* (23), 6983–6988.
- (21) Gangloff, N.; Fetsch, C.; Luxenhofer, R. *Macromol. Rapid Commun.* **2013**, *34* (12), 997–1001.
- (22) Aliferis, T.; Iatrou, H.; Hadjichristidis, N. *Biomacromolecules* **2004**, *5* (5), 1653–1656.
- (23) Kramer, J. R.; Deming, T. J. *Biomacromolecules* **2010**, *11* (12), 3668–3672.
- (24) Bailey, J. L. *J. Chem. Soc.* **1950**, No. Dec, 3461–3466.
- (25) Aubert, P.; Jeffreys, R. A.; Knott, E. B. *J. Chem. Soc.* **1951**, No. Aug, 2195–2197.
- (26) Kricheldorf, H. R. *Makromol. Chem.* **1974**, *175* (12), 3325–3342.
- (27) Kricheldorf, H. R.; Böisinger, K. *Makromol. Chem.* **1976**, *177* (5), 1243–1258.
- (28) Kricheldorf, H. R.; Sell, M.; Schwarz, G. *J. Macromol. Sci., Part A: Pure Appl. Chem.* **2008**, *45* (6), 425–430.
- (29) Tao, X. F.; Deng, C.; Ling, J. *Macromol. Rapid Commun.* **2014**, *35* (9), 875–881.
- (30) Guillaume, S. M.; Schappacher, M.; Soum, A. *Macromolecules* **2003**, *36* (1), 54–60.
- (31) Palard, I.; Soum, A.; Guillaume, S. M. *Macromolecules* **2005**, *38* (16), 6888–6894.
- (32) Gao, W.; Cui, D. M.; Liu, X. M.; Zhang, Y.; Mu, Y. *Organometallics* **2008**, *27* (22), 5889–5893.
- (33) Li, X.; Zhu, Y. H.; Ling, J.; Shen, Z. Q. *Macromol. Rapid Commun.* **2012**, *33* (11), 1008–1013.
- (34) Lin, J. O.; Chen, W. L.; Shen, Z. Q.; Ling, J. *Macromolecules* **2013**, *46* (19), 7769–7776.
- (35) You, L. X.; Shen, Z. Q.; Kong, J.; Ling, J. *Polymer* **2014**, *55* (10), 2404–2410.
- (36) Shang, X. M.; Liu, X. L.; Cui, D. M. *J. Polym. Sci., Polym. Chem.* **2007**, *45* (23), 5662–5672.
- (37) Zhao, W.; Cui, D. M.; Liu, X. L.; Chen, X. S. *Macromolecules* **2010**, *43* (16), 6678–6684.
- (38) Ling, J.; Shen, Z. Q.; Huang, Q. H. *Macromolecules* **2001**, *34* (22), 7613–7616.
- (39) Ling, J.; Zhang, Y. F.; Shen, Z. Q. *Chin. Chem. Lett.* **2001**, *12* (1), 41–42.
- (40) Palard, I.; Schappacher, M.; Belloncle, B.; Soum, A.; Guillaume, S. M. *Chem.—Eur. J.* **2007**, *13* (5), 1511–1521.
- (41) Ling, J.; You, L. X.; Wang, Y. F.; Shen, Z. Q. *J. Appl. Polym. Sci.* **2012**, *124* (3), 2537–2540.
- (42) You, L. X.; Hogen-Esch, T. E.; Zhu, Y. H.; Ling, J.; Shen, Z. Q. *Polymer* **2012**, *53* (19), 4112–4118.
- (43) You, L. X.; Ling, J. *Macromolecules* **2014**, *47* (7), 2219–2225.
- (44) Hu, X. P.; Wu, J.; Xu, Z. K.; Feng, L. X. *Chin. J. Polym. Sci.* **2000**, *18* (4), 369–372.
- (45) Ling, J.; Peng, H.; Shen, Z. Q. *J. Polym. Sci., Polym. Chem.* **2012**, *50* (18), 3743–3749.
- (46) Peng, H.; Ling, J.; Shen, Z. Q. *J. Polym. Sci., Polym. Chem.* **2012**, *50* (6), 1076–1085.
- (47) Peng, H.; Ling, J.; Zhu, Y. H.; You, L. X.; Shen, Z. Q. *J. Polym. Sci., Polym. Chem.* **2012**, *50* (15), 3016–3029.
- (48) Gibbs, T. J. K.; Boomhoff, M.; Tomkinson, N. C. O. *Synlett* **2007**, *10*, 1573–1576.
- (49) Kricheldorf, H. R.; von Lossow, C.; Schwarz, G. *Macromolecules* **2005**, *38* (13), 5513–5518.
- (50) Lutz, J. F.; Akdemir, O.; Hoth, A. *J. Am. Chem. Soc.* **2006**, *128* (40), 13046–13047.
- (51) Park, J. S.; Kataoka, K. *Macromolecules* **2007**, *40* (10), 3599–3609.
- (52) Hoogenboom, R.; Thijs, H. M. L.; Jochems, M. J. H. C.; van Lankvelt, B. M.; Fijten, M. W. M.; Schubert, U. S. *Chem. Commun.* **2008**, *44*, 5758–5760.